Ferroelectric surface chemistry: First-principles study of adsorption on the stoichiometric LiNbO₃ (0001) surface

Chen Yue [1] Xiaomei Lu,[1,2,*] Junting Zhang,[3] Fengzhen Huang,[1,2] and Jinsong Zhu[1]

[1]*National Laboratory of Solid State Microstructures and Physics School, Nanjing University, Nanjing 210093, People's Republic of China*
[2]*Collaborative Innovation Center of Advanced Microstructures, Nanjing University, Nanjing 210093, People's Republic of China*
[3]*Department of Physics, China University of Mining and Technology, Xuzhou 221116, People's Republic of China*

We present a first-principles study of stoichiometric LiNbO₃ (0001) clean positive and negative surface and with H_2O, OH and H adsorption. While we exclude internal compensation mechanisms such as enrichment or depletion of certain atomic species, in the frame of surface relaxation with constant stoichiometry and considering the foreign adsorbates, the structures with lowest energy states are obtained. We find that the positive stoichiometric surface compensates the surface charges by abnormal ion displacements. We also suggest that foreign adsorbates are in significantly different bonds with opposite polar surfaces, leading to diverse mechanisms of surface charge compensation. Water molecules adsorbed on negative surface may even alter the surface polarity. We refer to five mechanisms for the charge compensation and the stabilization of stoichiometric polar surfaces, that is, the bonding interaction between adsorbed atoms and surface ions, the dipole moment of adsorbates, the (abnormal) ion displacements-induced change of surface bound charge, the variation of surface spontaneous polarization, and the mobile carriers, with the priority lowering in turn.

I. INTRODUCTION

Ferroelectrics are a special subclass of piezoelectric materials that have spontaneous polarization remaining stable in the absence of external electric fields, and can be switched between two different states by applying a sufficiently large electric field [1]. With the increasing demand of applications ranging from optoelectronics to surface acoustic wave and to heterogeneous catalysis, and due to the development of fabrication and surface analysis technology [2–5], the polar surface of ferroelectric oxide has attracted more and more attention after the extensive study of ferroelectric bulk. Cutting ferroelectrics perpendicular to the polar axis results in two surfaces with opposite polarity, and the dipole moment associated with each repeat unit perpendicular to the surface leading to a thickness-dependent electrostatic energy that destabilizes surfaces [6]. The surface can be stabilized by compensating surface charges in several mechanisms, including deep modifications in surface morphology and stoichiometry by spontaneous atom desorption, faceting, surface reconstruction, and molecular adsorption, as well as fundamental changes of the electronic structure such as total or partial filling of electronic states [6–8].

Lithium niobate LiNbO₃ (LN) is a kind of artificial dielectric material with a trigonal crystal structure. Because of its excellent ferroelectric, piezoelectric, thermoelectric, and electro-optical properties, it has attracted much attention for a long time, and has been widely used in various fields such as nonlinear optics, optoelectronics, acoustics, and so on. As a uniaxial ferroelectric material, the polarization of LN is as high as $0.7 \, C/m^2$ along the hexagonal [0001] direction,

making the experimental study of the *z*-cut surface very challenging. The surface charge interfere with the measurement of scanning tunneling microscopy) or diffraction technology, and also high-resolution atomic force microscopy [9].

Theoretically, in 2008, Levchenko *et al.* [10] simulated the relative thermodynamic stability of LN (0001) polar surface of different stoichiometry within the density functional theory (DFT), predicting that the thermodynamically stable positive and negative surface should be quite different, namely, Li_2-O_3-Nb- terminal and -Nb-Li-O, respectively. The analysis using a simple ionic model based on the modern theory of polarization revealed that surface charge passivation by ions is favored over the passivation by mobile carriers, which well explained the ion evaporation on the polar surface [11]. However, other reports indicated that, although surface reconstruction dominates the compensation of surface charge at temperatures higher than 870 K, the foreign adsorbates are the main contributors on the LN (0001) polar surface at lower temperatures [12,13].

The adsorption of a series of common molecules and radicals on the LN (0001) surfaces has been modeled by different groups via DFT [14–17]. These substances have various adsorption energy on positive and negative surfaces, ranging from low energies for physisorption (<1 eV) to high energies indicating chemisorption (>1 eV) [7]. While CO molecules and H radicals are more likely adsorbed on the positive surface, others, such as N_2, O_2, CO_2, CH_4, H_2, N_2O, H_2O molecules and OH radicals, tend to adsorb on the negative surface [15]. All these works demonstrate that adsorption behaviors not only depend on the foreign species, but more importantly, can be greatly affected by the polarity of the ferroelectric surface.

*xiaomeil@nju.edu.cn

Due to the technological advances in recent years, breakthrough has been achieved in the experimental observation of the polar surface [18,19]. Multiple physical and chemical processes are proposed to occur on the ferroelectric surfaces with molecule/ion adsorption, leading to a more complex scenario such that the surface polarization may be affected [20]. Among these common adsorbates, the water molecule is prominent because of its presence and influence on the polar surface unless in ultrahigh vacuum, and a variety of applications including hydrogen product, electrochemistry analysis, biochemical cell, etc. [21]. Different reports have shown that ambient humidity (the number of water molecules adsorbed on the surface) determined the size of abnormally switched ferroelectric domains [21–23]. And the images of LN (0001) polar surface in atomic resolution have only been obtained in aqueous solution [24]. Kumara *et al.* demonstrated the presences of OH and H dissociated from water molecules adsorbed at LN(0001) polar surface [9], and it is also considered that OH and H participate in the polarization reversal of a ferroelectric surface via a polarization-coupled electrochemical process [18].

These works reveal that the foreign adsorbates have a significant effect on the properties of ferroelectric surface, and play very important roles in the surface stabilization. Up to now, most of the theoretical investigations of adsorptions on LN (0001) polar surfaces depend on thermodynamically stable surfaces which are nonstoichiometric. In this case, it is difficult to discuss the influence of the foreign adsorbates on a polar surface. To get a similar result as the surface polarization reversal in the experiment [21–23], we consider the surface relaxation as the only inner compensation mechanism without varying the stoichiometry, and then find the structures with lowest energy states while considering foreign adsorbates.

In this work, we simulated the H_2O, OH and H adsorbed on stoichiometric LN (0001) positive and negative surfaces by first-principles calculations. We determine the adsorption energy, adsorption sites and configurations, and analyze the geometry and electronic structure of the LN surface. We suggest that these adsorbates are in significantly different bonds with opposite polar surfaces, leading to diverse mechanisms of surface charge compensation. Water molecules adsorbed on negative surface may even alter the surface polarity. This work reveals the mechanisms underlying the surface stabilization, as well as the interaction of these common adsorbates with polar surfaces.

II. METHODOLOGY

The calculation of DFT based on the augmented plane wave method is implemented in VASP [25,26]. The generalized gradient approximation described by Perdew *et al.* [27] is used to treat exchange correlation terms, which explicitly includes valence electrons in Li $2s$, Nb $4p5s4d$, O $2s2p$ and H $1s$ orbits. The cutoff energy of plane wave is set to 500 eV.

This work is based on the single-domain LN ferroelectric optical crystal with a spontaneous polarization along the (0001) direction. LN (0001) stoichiometric polar surfaces are simulated by nine -Li-O_3-Nb- trilayer structure (45 atoms) with a vacuum region ~16 Å and 2 × 2 surface periodicity, in which -Li-O_3-Nb- trilayers are regarded as a basic structure (see Fig. 1). The atomic positions of
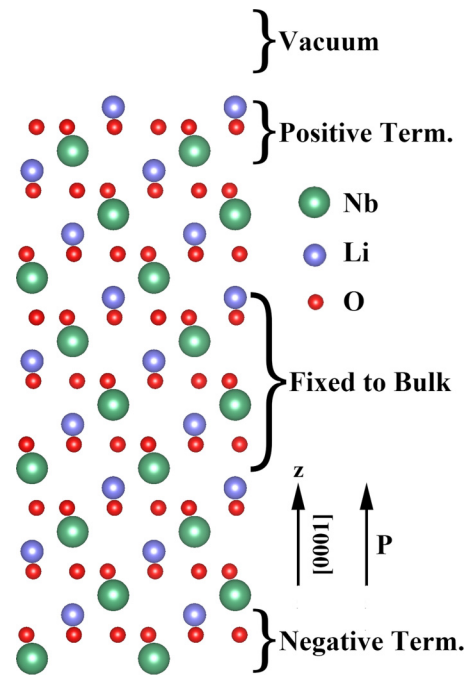

FIG. 1. Schematic representation of simulation cell, shown for a positive terminated surface, bulk, and a negative terminated surface.

the three -Li-O_3-Nb- trilayers in the middle are fixed to the bulk value. The other atoms in upper and lower three -Li-O_3-Nb- trilayers and external adsorbates are allowed to relax in all directions, until the force on each ion is less than 0.02 eV/Å. A 3 × 3 × 1 Monkhorst-Pack k-point grid is adopted for Brillouin zone integral. As there is no experimental evidence of LN surfaces with net spin moment, we restrict ourselves to spin-unpolarized calculations. The dipole correction [28,29] is used to eliminate spurious electrostatic coupling between periodic copies in the z direction.

After the calculation of clean surface, we then add foreign adsorbates such as H_2O, OH, and H on the surface. These foreign substances are regarded as "internal atoms" of the whole system and participate in the relaxation to an equilibrium state.

III. RESULTS AND DISCUSSION

A. Clean LN (0001) positive and negative surfaces

In order to identify the mechanisms of the surface charge compensation in the absence of foreign adsorbates, we first study the geometry and electronic structure of clean LN (0001) positive and negative surface. As shown in Fig. 2, both terminals of positive and negative surfaces show certain ionic displacements relative to the bulk structure. The positive surface changes from Li-O_3-Nb-terminal to Li_2-O_3-Nb-terminal [see Fig. 2(a)], similar to that in Ref. [10], while the negative surface shows less structure modification [see Fig. 2(c)]. Detailed analysis is as follows.

1. Clean positive surface

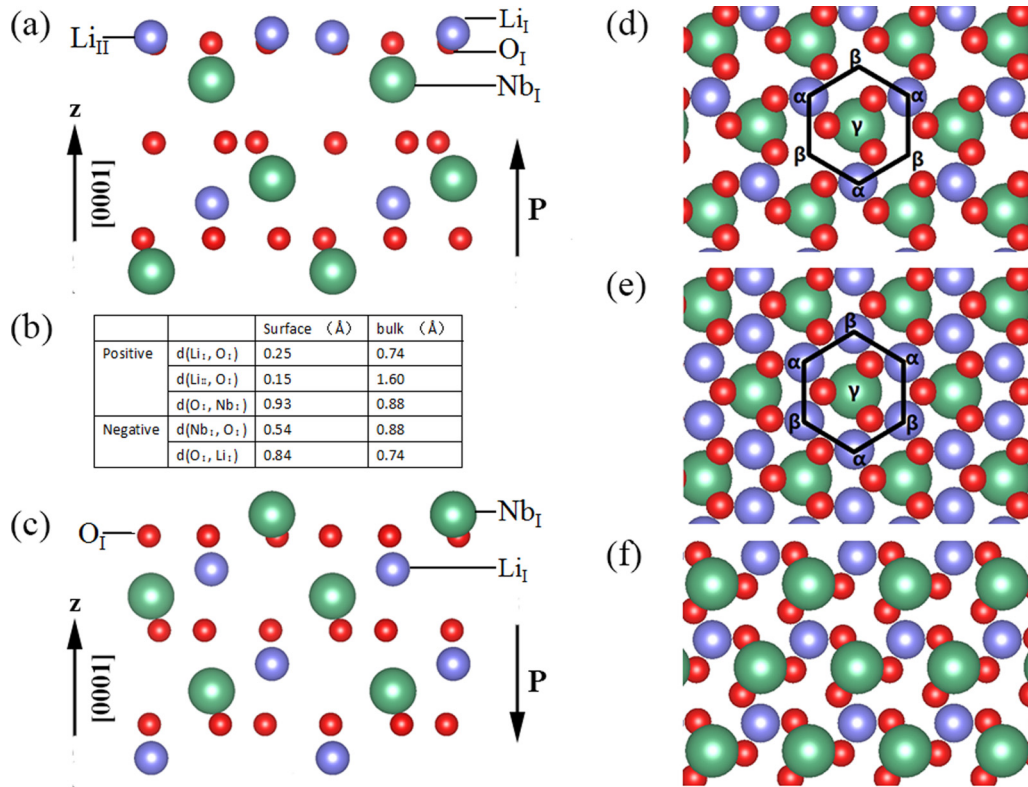At LN (0001) positive surface, compared with the bulk value, the outermost Li_I ions show large inward (contrary to

FIG. 2. Side view of the stoichiometric clean positive (a) and negative (c) LN(0001) surface. Distance (Å) between the atomic layers of the stable surfaces with bulk values for comparison in (b). Top view of the clean positive LN(0001) surface before (d) relaxation (same to the bulk layer) and after (e) relaxation, a hexagon in the graph is chosen as a basic cell, with the Li-O_3- corner, O_3- corner, and the center O_3-Nb-structure marked as α, β, and γ, respectively. Top view of the clean negative LN (0001) surface (f).

the polarization direction) relaxation of 0.49 Å and remains above the oxygen plane, and Nb_I ions also shift inward relaxation of only 0.05 Å. At the same time, the Li_{II} ions that belong to the secondary -Li-O_3-Nb- trilayer shift 1.75 Å outward (same as the polarization direction) to the top of the outer oxygen layer from below. The effect of ion displacements on the surface polarization can be estimated from Figs. 2(a) and 2(b). The displacements of the outmost Li_I and Nb_I ions are opposite to the polarization direction, tending to reduce the polarization. Although the Li_{II} ions with positive charges move from the second trilayer to the outmost trilayer, which succeedingly increase the local polarization of the outermost trilayer, the overall polarization is still decreasing in the outermost trilayer because of the small distance between Li_{II} ions and neighboring oxygen plane. Compared with the work by Sanna *et al.* [30], our calculations show the Li vacancy in secondary trilayer and the difference in the positions of Li_I and Li_{II} ions. The Li_I ions are much closer to the outer oxygen plane, and the Li_{II} ions are above instead of below the oxygen plane.

To explain the abnormal displacement of Li_{II} ions, we further analyzed the distribution of bound charges on the LN surface by introducing an ionic model based on the formal oxidation state Nb^{5+}, Li^+, and O^{2-} [10]. The top view of the clean LN (0001) positive surface before and after relaxation is shown in Figs. 2(d) and 2(e), and for the sake of comparison, a hexagon in the graph is chosen as a basic cell, with the Li-O_3-corner, O_3- corner, and the center O_3-Nb- structure marked as

α, β, and γ, respectively. Before relaxation, the total $-5e/2$ charge of the hexagonal cell is nonuniformly distributed, with $-e/3$ at each α, $-2e/3$ at each β and $+e/2$ at each γ [see Fig. 2(d)]. The displacements of Li_I and Nb_I ions contribute to the compensation of surface bound charge in total, however, they further increase the roughness of charge distribution, as more positive charge introduced at α and γ, and no changes at β. After relaxation, Li_{II} ions with positive charges move to the outmost trilayer at β. By forming the similar Li-O_3- structure as α, they not only compensate the previous negative charge at β, but also lower the roughness of charge distribution on the terminal. According to the analysis before, the displacements of Li_I and Nb_I ions decrease the partial polarization at α and γ, while Li_{II} ions introduce a small positive polarization at β. These movements lower the polarization contribution to the compensation of surface charge, and yet make the total surface polarization and in turn the surface charge distribution more uniform.

Considering the contribution of mobile carriers, the layer-resolved density of states (LDOS) on the clean LN (0001) positive and negative surfaces after relaxation is shown in Fig. 3. It can be seen that the inner part (middle blue part) remains insulated, while the Fermi level passes through the valence-band maximum (VBM) in the two outer layers (upper red part), leading to holes on the positive surface states. These holes in valence band could compensate the negative surface bound charges [8]. Therefore, mobile carriers associated with displacements of ions on positive
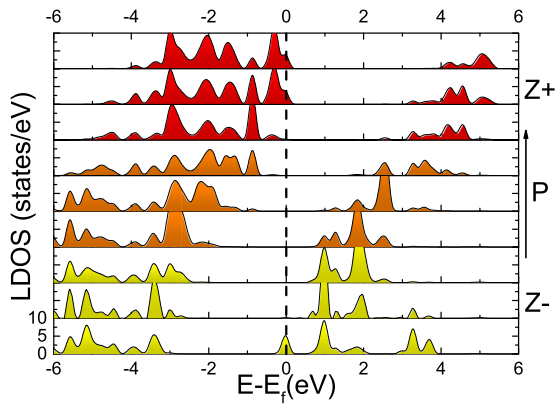
FIG. 3. Layer-resolved density of states (LDOS) for the clean LN(0001) surface, the red, yellow, and orange regions denote positive surface, negative surface and bulk, respectively.

surfaces contribute to the passivation of surface charge as well.

The above analysis indicates that the obvious ion displacements of the clean LN(0001) positive surface (compared to the bulk) results in the change of bound charge, electronic displacement polarization, and mobile carriers transformation, thus eventually makes the surface charge distribution more uniform and passivated.

2. Clean LN (0001) negative surfaces

In the case of a clean LN (0001) negative surface (before relaxation, see Fig. 1), with a Nb termination, the overall surface charge distribution is relatively uniform with bound charges of $+5/2e$ around each Nb ions [10]. The negative charges brought by polarization compensate the surface charge to a certain extent.

After relaxation, the outermost Nb_I ions shifts 0.34 Å inward (same to the polarization direction), while they remain above the oxygen plane, and the Li_I ions shifts 0.1 Å inward (same to the polarization direction) as well [see Figs. 2(b), 2(c), and 2(f)]. These ion displacements increase the surface polarization, and compensate more surface charges.

According to the LDOS in Fig. 3, for the layers within the subouter layer, the Fermi level is just in the band gap, suggesting the absence of mobile carriers. Nevertheless, for the outmost layer, a new peak arising near the bottom of conduction band is passed through by the Fermi level, indicating the presence of free electrons that could screen part of the positive surface bound charges [8]. Note that the trend of the DOS on the positive and negative surfaces shown in Fig. 3 is similar to that in the supplementary in Ref. [31] on the thermodynamically stable LN surfaces.

Comparing the clean LN (0001) positive and negative surface, we demonstrate that charge compensation mechanisms depend highly on the surface polarity. At the positive surface, the surface charge compensation is mainly caused by the abnormal displacement of Li ions, the weakened ferroelectric polarization, and the holes entering valence-band states, with their priority decreasing in turn. While at the negative surface, the enhanced ferroelectric polarization and the electrons entering the conduction-band states dominate the surface charge compensation.

B. Adsorption on positive surface

We then model the adsorption of H_2O, OH, and H on the above relaxed LN (0001) positive and negative surfaces. To distinguish the binding form between the foreign adsorbates and the surface, the adsorption energy are calculated as

$$E_{ads} = E_{total} - E_{slab} - E_{gas}. \qquad (1)$$

E_{total}, E_{slab}, and E_{gas} are the total energies of adsorption structure, the clean LN surface, and the adsorbed molecules in gas phase, respectively.

1. H_2O adsorption

With water adsorption, the positive surface transform from Li_2-O_3-Nb- terminal back to Li-O_3-Nb- terminal, which is similar to that of clean surface before relaxation [see Fig. 4(a)]. By contrast with the relaxed clean surface, the outermost Li_I ions shift outward (same to the polarization direction) by 0.38 Å from the position close to the oxygen plane to 0.63 Å above the plane, which is 0.11 Å smaller than the bulk value. The Nb_I ions return to the position of 0.87 Å below the oxygen plane, similar to the bulk value with a difference of only 0.01 Å. The Li_{II} ions, formerly located above the outermost oxygen plane to constitute the Li_2-O_3-Nb- terminal, shift inward (contrary to the polarization direction) to the position of 1.10 Å below the outmost oxygen plane, 0.5 Å smaller than the bulk value. It shows that the bound charge distribution of the surface with adsorbed H_2O is the same as that of the clean surface before relaxation. Compared with polarization of clean surface before relaxation, the polarization produced by Li_I ion displacements are slightly smaller, while the case of Nb_I ions are almost the same, and both are greater than that of clean surface after relaxation. The Li_{II} ions return to below the Nb_I ions, making the former abnormal displacements disappear, and contribute little to the polarization of the outmost trilayer. In total, the surface polarization is smaller than that of clean sample before relaxation, while larger than that after relaxation.

The LDOS in Fig. 5(a) shows that the Fermi level also passes through VBM in the two outer layers as a relaxed clean surface, containing more holes in the valence-band states in the outermost layer while less holes in the subouter layer.

We further analyze the contribution of H_2O to surface charge compensation from Fig. 4(b). The H_2O adsorbs on the positive surface between the outermost Li_I ion and a neighboring O_I ion, with atomic distance $d(O\text{-}Li_I) = 2.06$ Å. One of the two H atoms points to the surface with atomic distance $d(H\text{-}O_I) = 1.92$ Å, while the other H atom points to the vacuum along the O-H bond. The dipole moment of H_2O, obliquely pointing to the surface, is against the surface polarization in (0001) direction, which partially offsets the surface dipole moment and helps to stabilize the surface.

The adsorption energy of 0.58 eV (<1 eV) also indicates the physisorption of H_2O on the positive surface. The charge redistribution [see Fig. 4(c)] shows no charge transfer between O atom in H_2O and Li_I ion, but charge accumulates over the Li_I ion because of the existence of a lone pair electrons from O atom, thus forming an oxygen tetrahedron-like structure with Li-O_3- on the surface [(dot line in Fig. 4(c)]. Differently, there
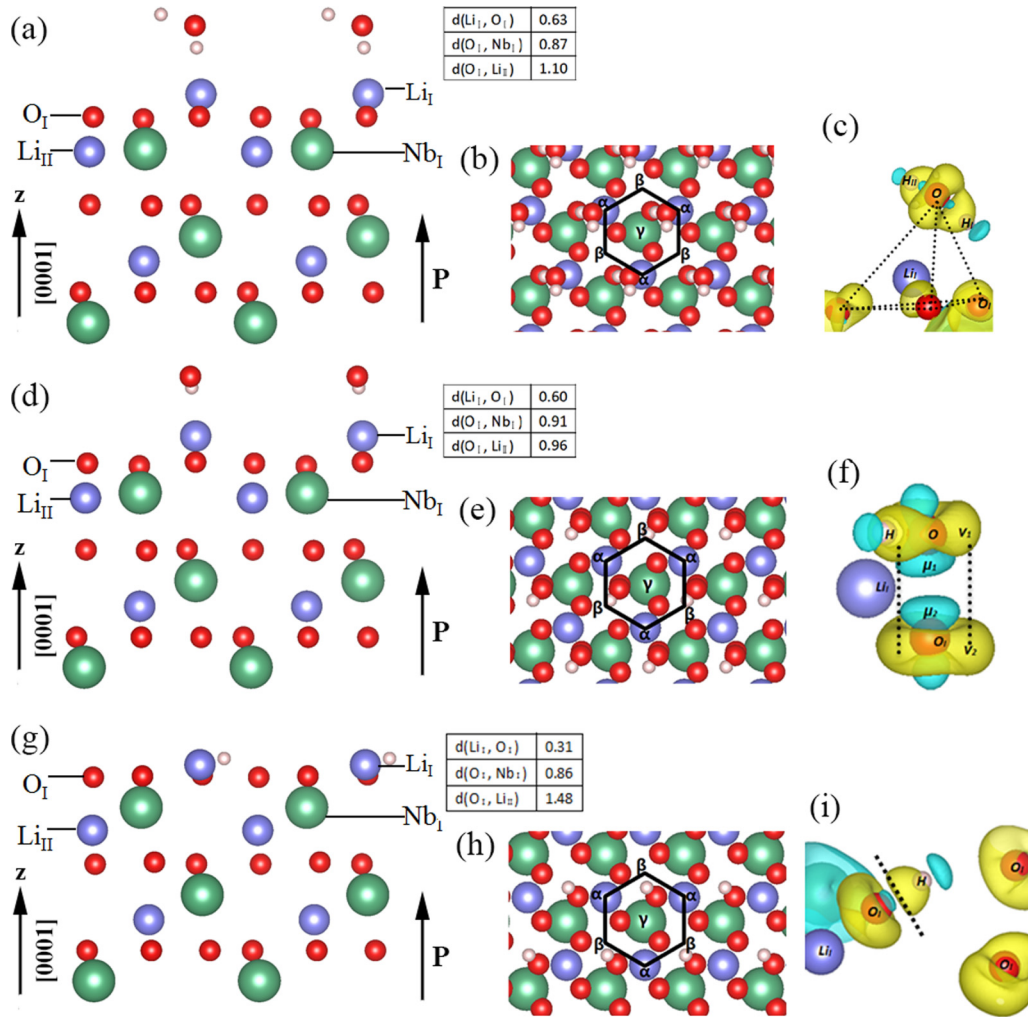
FIG. 4. Side view, top view and charge redistribution of the positive LN(0001) surface with H_2O[(a), (b), and (c)], OH[(d), (e), and (f)] and H[(g), (h), and (i)] adsorption. H is in pink (other colors the same as Fig. 1). Regions in yellow indicate charge accumulation, and regions in blue indicate charge depletion.

is more charge depletion between H_{II} atom and nearest O_I ion, compared with H_I, suggesting a weak hydrogen bonding between H_{II} atom and nearest O_I ion.

Referring to the previous analysis about bound charges on positive surface, the O atom in the adsorbed H_2O molecular supply additional negative charges at α, making the bound charge distribution at α close to that at β [Fig. 4(b)]. Meanwhile, more charge depletion near the H_{II} atom [Fig. 4(c)] means the H_{II} atom provides positive charges at β, also makes the surface charges distribution more uniform.

Generally speaking, after water adsorption, the ion positions in the surface layer are similar to those of bulk crystals, without any abnormal ion displacements as the clean positive surface. The dipole moment of adsorbed H_2O is opposite to the surface polarization in (0001) direction, and positive charges are introduced to compensate the negative bound charges on the surface, with the effect weaker than that of the aforementioned abnormal ion displacements. In this case, the surface spontaneous polarization and mobile carriers are greater and contribute more to surface charge compensation than the case of clean positive surface after relaxation.

2. OH adsorption

The structure of the LN (0001) positive surface with OH adsorbed is similar to that of H_2O adsorbed, with slight differences in atomic distances [see Fig. 4(d)]. The relative displacements of Li_I and Nb_I ions are only about 0.03 Å, while the Li_{II} ions are closer to the outermost oxygen plane with relative displacement about 0.14 Å, and all these displacements are against the surface polarization. The bound charge distribution is consistent with the cases of the positive surface before relaxation and with H_2O adsorbed, while the overall polarization is greater than that of the clean positive surface after relaxation but still slightly less than that with H_2O adsorbed. The LDOS of positive surface with OH adsorbed is similar to that of H_2O adsorbed, as shown in Fig. 5(b), with fewer holes entering the valence-band states.

From the top view [see Fig. 4(e)], we can see that the adsorbed OH are located above β, with the distance between O atoms and neighboring O_I ions of $d(O\text{-}O_I) = 1.49$ Å, while the H atoms are far from the surface ions, with the dipole moment of OH perpendicular to the surface polarization. The adsorption energy of OH on positive surface is 3.20 eV,
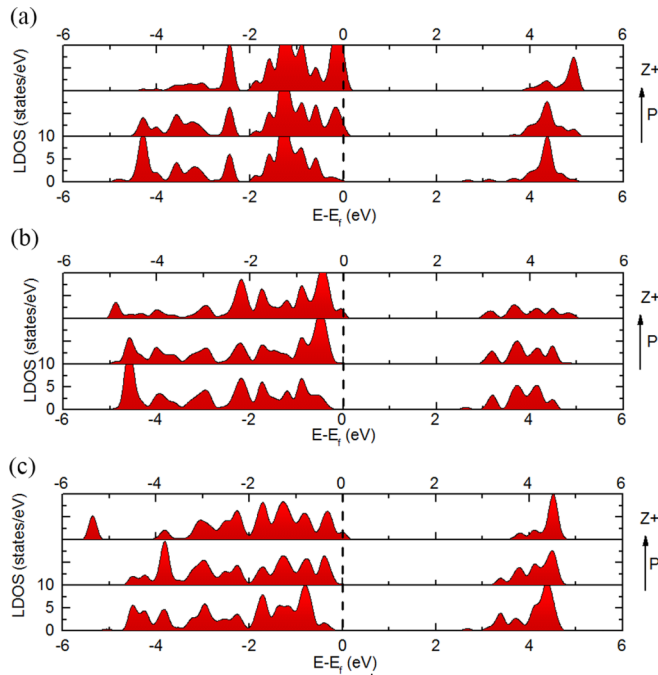
(a)

(b)

(c)

FIG. 5. Layer-resolved density of states (LDOS) on the LN (0001) positive surface with H_2O(a), OH(b), and H(c) adsorption.

larger than 1 eV and suggesting a chemisorption. The charge redistribution [see Fig. 4(f)] shows that charge consumes at μ_1 and μ_2, and then accumulates at ν_1 and ν_2 near the O atom and O_I ion, respectively, indicating the formation of a parallel π bond between the O atom and O_I ion [dotted line in Fig. 4(f)]. The existence of the O-O covalent bond (π bond) could be further confirmed by the bond length $d(\text{O-O}_I) = 1.49\,\text{Å}$ similar to that of the H-O-O-H bond (1.48 Å) in Ref. [32]. As to the surface bound charge distribution, OH consumes part of the negative bound charges at β through O-O covalent bonds, making the surface charge distribution more uniform.

Generally speaking, after adsorption of OH, the surface geometry is similar to that with H_2O adsorbed. As forming covalent bonds, OH contributes more to surface charge compensation than H_2O, while surface spontaneous polarization and mobile carriers contribute less.

3. H adsorption

The structure of LN (0001) positive surface adsorbed with H atoms [see Fig. 4(g)] is similar to that of H_2O and OH adsorbed, except for the differences in the specific atomic distances. The outermost Li_I ions shift inward (contrary to the polarization direction) to the position of 0.31 Å above the oxygen plane, much lower than that with H_2O and OH adsorbed, while the position of Nb_I ions remain almost unchanged. The Li_{II} ions also shift inward to 1.48 Å below the outermost oxygen plane, which is 0.12 Å lower than that of H_2O adsorbed. After H adsorption, the surface bound charge distribution is consistent with the case of H_2O and OH adsorption as well as the clean positive surface before relaxation. However, the polarization induced by the displacements of Li_I ions is greatly reduced, which is similar to that of the positive surface after relaxation. The LDOS [see Fig. 5(c)] reveals that

the holes present in the outermost and suboutermost layers are similar to the case of OH adsorption, while fewer than the case of H_2O adsorption.

From the top view [Fig. 4(h)], it can be seen that the absorbed H atoms are located above β, and the distance between the H atoms and the nearest O_I ions is $d(\text{H-O}_I) = 0.98$ Å. The 5.16-eV adsorption energy of H atom, much larger than 1 eV, suggests that H atoms are also chemically adsorbed at the positive surface. The H-O covalent bonds are formed as confirmed by the charge accumulation just in the middle of the H atom and O_I ion [see Fig. 4(i) dot line], with the bond length equal to that in water molecule. Thus the H atom introduces a charge of $+e/3$ at β, compensating the surface charge and making the charge distribution more uniform.

For the H atoms adsorption, the covalent bond between H atom and outermost O_I ion is stronger than the case of OH atom, which contributes more to surface charge compensation. Although the surface geometry is similar to that of OH adsorption, the atomic distances are quite different. In this case, the surface spontaneous polarization significantly reduces, so as to compensate for the much fewer surface charges, while the contribution from mobile carriers is similar for H and OH cases.

C. Adsorption on negative surfaces

Next, we investigate the adsorption of H_2O, OH and H on the LN (0001) negative surface. As Fig. 6 shows, the negative surface exhibits different characters from the positive one.

1. H_2O adsorption

After H_2O adsorption on the negative surface, the terminal undergoes a great transformation [see Fig. 6(a)]. Compared with the clean negative surface, the outermost Nb_I ions shift inward from the position above the oxygen plane to 0.86 Å below. At the same time, the Li_I ions under the oxygen plane shift outward to a position 0.67 Å above the oxygen plane. Thus the overall structure is similar to that of the positive surface with H_2O adsorbed. These results indicate the structure reconstruction at the negative terminal after H_2O adsorption, with Nb-O_3-Li terminal changing to the Li-O_3-Nb-terminal, and the bound charges alter from positive to negative accordingly. In the subouter layer, Nb_{II} ions shift 0.12 Å outward, while Li_{II} ions shift 0.49 Å inward, both away from the second oxygen plane in opposite directions. In this case, Nb_{II} ions and the outermost Nb_I ions are very close, so that they provide more positive charges to passivate and balance the surface charges in the outermost layer. In terms of polarization change, the outermost layer reverses from negative polarization to positive polarization, almost equivalent to the positive surface with H_2O adsorbed. The polarization of the subouter layer was decreased by the outward shifts of Nb_{II} ions, while increased by the inward shifts of Li_{II} ions. Therefore, from the outermost layer to the interlayer and then to the subouter layer, the polarization changes from positive to less negative and then to more negative. The LDOS in Fig. 7(a) shows that Fermi level passes through conduction band maximum (CBM) in both the outer and the subouter layers, indicating the presence of electrons in the conductive-band states to compensate the surface charges.
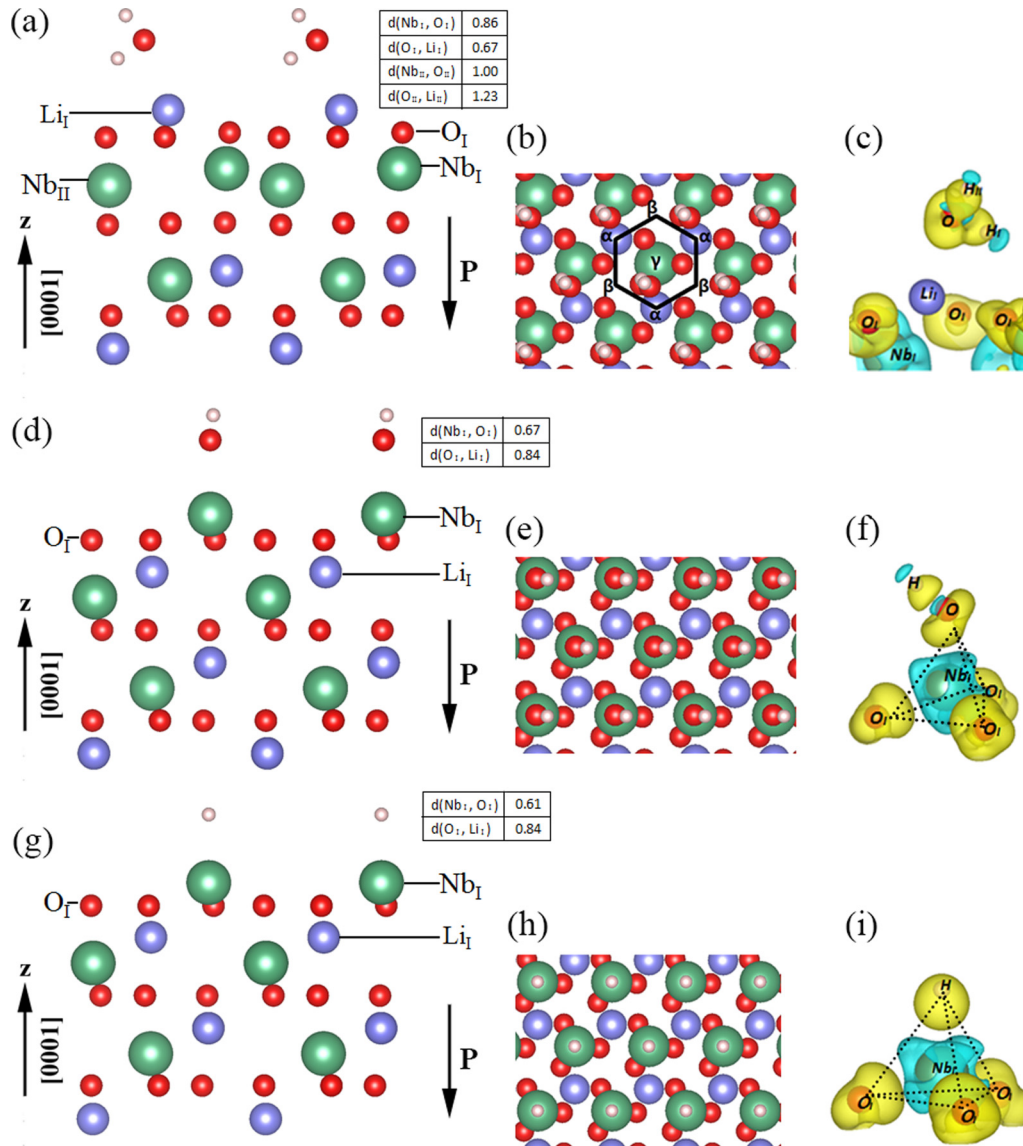
d(Nb$_I$, O$_I$)	0.86
d(O$_I$, Li$_I$)	0.67
d(Nb$_{II}$, O$_{II}$)	1.00
d(O$_{II}$, Li$_{II}$)	1.23

d(Nb$_I$, O$_I$)	0.67
d(O$_I$, Li$_I$)	0.84

d(Nb$_I$, O$_I$)	0.61
d(O$_I$, Li$_I$)	0.84

FIG. 6. Side view, top view and charge redistribution of the negative LN(0001) surface with H$_2$O[(a), (b), and (c)], OH[(d), (e), and (f)] and H[(g), (h), and (i)] adsorption. Color coding as in Fig. 4.

From the top view [see Fig. 6(b)], it can be seen that the adsorbed H$_2$O locates between the top Li$_I$ ion and the O$_I$ ion, similar to the case of the positive surface, with slight differences in atomic distances. The distance between the O atom in H$_2$O and the Li$_I$ ion is d(O-Li$_I$) = 2.03 Å. One of the two H atoms is located above the O$_I$ ion, with a distance of d(H-O$_I$) = 2.08 Å, being 0.16 Å longer, and the other points outward to the vacuum along the O-H bond. In this configuration, the dipole moment of H$_2$O obliquely points outward, parallel to the polarization of the reversed negative terminal in the (0001) direction, thus providing negative charges to the surface.

The adsorption energy of H$_2$O on the negative surface is 1.43 eV. Although the adsorption energy is larger than 1 eV, it does not mean a chemisorption, since the energy is correlated with the switching of the surface as aforementioned. The charge redistribution [see Fig. 6(c)] is approximately the same as that of the H$_2$O-adsorbed positive surface. Both the negative charge from O atoms at α and the positive charges

from H atoms at β (through weak hydrogen bonding) make the surface charge distribution more uniform [Fig. 6(b)].

Generally speaking, after H$_2$O adsorption, surface reconstruction exhibits at the negative surface. The polarization of the outermost layer switches 180° and becomes parallel to the dipole moment of H$_2$O in (0001) direction, which causes the change of bound charges, spontaneous polarization, and mobile carriers, and finally ensures the stability of the reconstructed surface. This result is consistent with the previous report, where the abnormal positive domain was observed in the center of negative domain written by piezoresponse force microscopy [33], with the abnormal domain size positively associated with the environmental humidity (i.e., the number of H$_2$O adsorbed on the surface) [22,23].

2. OH adsorption

The LN (0001) negative surface does not change much after OH adsorption [see Fig. 6(d)]. Compared with the clean
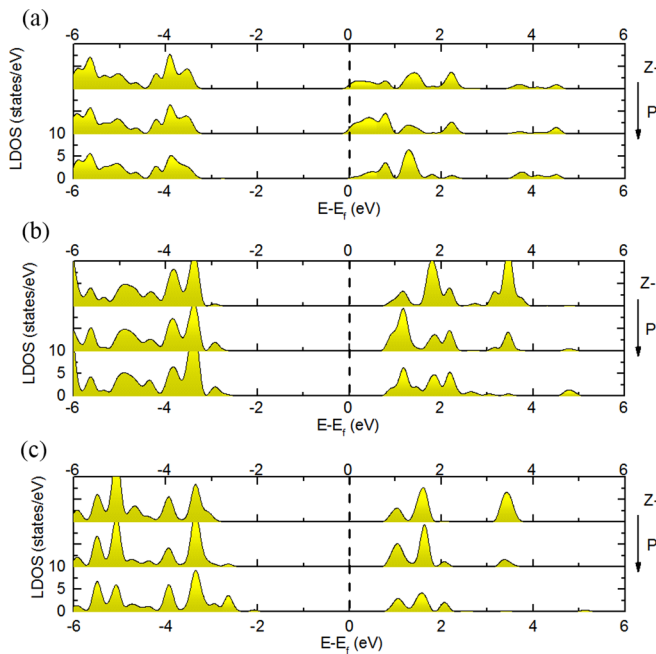
(a)

(b)

(c)

FIG. 7. Layer-resolved density of states (LDOS) on the LN (0001) negative surface with H_2O(a), OH(b), and H(c) adsorption.

negative surface after relaxation, almost all the ions keep still except for the outermost Nb_I ions moving outward (contrary to the polarization direction) by 0.13 Å. Thus the bound charge distribution of the OH-adsorbed negative surface is basically the same as that of the clean negative surface, while the spontaneous polarization is slightly weakened. The LDOS [see Fig. 7(b)] shows that the Fermi level no longer passes through the CBM of the outmost layer, thus there are no mobile carriers.

From the top view [see Fig. 6(e)], it can be seen that the O atoms in the adsorbed OH are right above the outermost Nb_I ion with a distance of d(O-Nb_I) = 1.94 Å, and the H atoms point obliquely to the vacuum along the O-H bond. Unlike on the positive surface, the dipole moment of OH on the negative surface is opposite to the overall polarization of the crystal in the (0001) direction. The adsorption energy of OH on the negative surface is 6.25 eV, even larger than that of OH on positive surface (3.20 eV), which also indicates a chemical adsorption. Figure 6(f) demonstrates charge depletion near the Nb_I ion, while charge accumulation near the O atom, suggests an ionic bond between Nb_I ion and O atom with bond length similar to the Nb-O bond in bulk. The formation of the ionic bond, leading to an oxygen tetrahedron-like structure with Nb-O_3- on the surface [dotted line in Fig. 6(f)], can effectively compensate for the positive surface bound charge.

In general, the adsorbed OH has a strong passivation effect on the negative polar surface through both the dipole moment opposite to the surface polarization and the formation of O-Nb_I ionic bond. Compared with the clean negative surface, only the outermost Nb_I ion moves outward after OH adsorption, resulting in less contribution of surface spontaneous polarization to charge compensation, and the mobile carriers disappear completely.

3. H adsorption

The structure of LN (0001) negative surface adsorbed with H atom is almost the same as that adsorbed with OH [see Fig. 6(g)], except for the outermost Nb_I ion moving 0.06 Å inward. Although the surface spontaneous polarization is slightly enhanced, the distribution of surface bound charges and the LDOS [see Fig. 7(c)] are both similar to those of OH adsorbed.

The adsorbed H atom is located right above the outermost Nb_I ion with a distance of d(H-Nb_I) = 1.78 Å, [see Fig. 6(h)]. The adsorption energy of H on the negative surface is 3.57 eV, also indicating chemical adsorption, though a bit weaker than that on the positive surface (5.16 eV). The charge redistribution [see Fig. 6(i)] illustrates the formation of H-Nb_I ionic bond (rather than covalent bond) with electrons accumulating near the H atom. It seems that, similar to OH adsorption, the adsorbed H atom could also effectively compensate the positive bound charges on the LN surface.

Briefly speaking, compared with the OH adsorption on negative surface, the charge compensation of the H adsorption is less because of the absence of external dipole moment and the weaker bonding between the adsorbed atoms and the surface ions. As for the LN surface, the contribution of the surface spontaneous polarization to charge compensation increases slightly due to the inward shift of Nb_I ion, while the mobile carriers are completely absent similar to the case of OH adsorption.

IV. CONCLUSION

We simulate the structure of stoichiometric LN (0001) clean positive and negative surface and with H_2O, OH, and H adsorption by first-principles DFT calculations. While we exclude internal compensation mechanisms such as enrichment or depletion of certain atomic species, in the frame of surface relaxation with constant stoichiometry and considering the foreign adsorbates, the structures with lowest energy states are obtained. For a clean LN (0001) polar surface, the mechanisms of surface charge compensation include the change of the surface bound charge, the variation of spontaneous polarization, and the mobile carriers. The change of surface bound charge caused by abnormal ion displacements are decisive on the positive surface, while the variation of spontaneous polarization and the mobile carriers become more important on the negative surface. H_2O are physically adsorbed on both the positive and negative surface. For surface charge compensation, the dipole moments of H_2O play a key role, which can even induce the reconstruction of the structure and the inversion of polarization in the outmost layer of negative surface, while the variation of surface spontaneous polarization and the mobile carriers are supportive. OH and H atoms are chemically adsorbed on LN (0001) polar surfaces, with covalent bonds on positive surfaces and ionic bonds on negative surfaces, respectively. The formation of chemical bonding dominates the stability of surface, while the contribution of surface spontaneous polarization and mobile carriers are greatly reduced, and mobile carriers are even absent in the presence of ionic bond.

All in all, we could refer to five mechanisms for the charge compensation and the stabilization of stoichiometric polar surfaces, that is, the bonding interaction between adsorbed atoms and surface ions, the dipole moment of adsorbates, the (abnormal) ion displacements-induced change of surface bound charge, the variation of surface spontaneous polarization, and the mobile carriers, with the priority lowering in turn. It should be noted that these results are obtained on the stoichiometric LN (0001) polar surfaces with no enrichment or depletion of certain atomic species. Although we can also obtain the same terminal on a clean positive surface as the thermodynamically stable terminal in Refs. [10,30], further work in comparing thermodynamic stabilities and the compensation mechanisms of different surface terminations (with different adsorbates and different changes in stoichiometry) are expected.

[1] K. A. Rabe, M. Dawber, C. Lichtensteiger, C. H. Ahn, and J. M. Triscone, Top. Appl. Phys. **105**, 1 (2007).

[2] A. Gruverman and A. Kholkin, Rep. Prog. Phys. **69**, 2443 (2006).

[3] S. V. Kalinin, A. Rar, and S. Jesse, IEEE Trans. Ultrason. Ferroelectric. **53**, 2226 (2006).

[4] A. Gruverman and S. V. Kalinin, J. Mater. Sci. **41**, 107 (2006).

[5] N. Balke, I. Bdikin, S. V. Kalinin, and A. L. Kholkin, J. Am. Ceram. Soc. **92**, 1629 (2009).

[6] K. Garrity, A. M. Kolpak, S. Ismail-Beigi, and E. I. Altman, Adv. Mater. **22**, 2969 (2010).

[7] S. Sanna and W. G. Schmidt, J. Phys.: Condens. Matter **29**, 413001 (2017).

[8] K. Garrity, A. Kakekhani, A. Kolpak, and S. Ismail-Beigi, Phys. Rev. B **88**, 045401 (2013).

[9] K. Cordero-Edwards, L. Rodriguez, A. Calo, M. J. Esplandiu, V. Perez-Dieste, C. Escudero, N. Domingo, and A. Verdaguer, J. Phys. Chem. C. **120**, 24048 (2016).

[10] S. V. Levchenko and A. M. Rappe, Phys. Rev. Lett. **100**, 256101 (2008).

[11] A. Y. Lushkin, V. B. Nazarenko, K. N. Pilipchak, V. F. Shnyukov, and A. G. Naumovets, J. Phys. D **32**, 9 (1999).

[12] S. Sanna, S. Rode, R. Hölscher, S. Klassen, C. Marutschke, K. Kobayashi, H. Yamada, W. G. Schmidt, and A. Kühnle, Phys. Rev. B **88**, 115422 (2013).

[13] S. Sanna, R. Holscher, and W. G. Schmidt, Appl. Surf. Sci. **301**, 70 (2014).

[14] R. Holscher, S. Sanna, and W. G. Schmidt, Phys. Status Solidi. C **9**, 1361 (2012).

[15] R. Holscher, W. G. Schmidt, and S. Sanna, J. Phys. Chem. C **118**, 10213 (2014).

[16] A. Riefer, S. Sanna, and W. G. Schmidt, Phys. Rev. B **86**, 125410 (2012).

[17] S. Sanna, R. Hölscher, and W. G. Schmidt, Phys. Rev. B **86**, 205407 (2012).

[18] E. Strelcov, A. V. Ievlev, S. Jesse, I. I. Kravchenko, II, V. Y. Shur, and S. V. Kalinin, Adv. Mater. **26**, 958 (2014).

[19] D. C. Coffey and D. S. Ginger, Nat. Mater. **5**, 735 (2006).

[20] S. V. Kalinin, D. A. Bonnell, T. Alvarez, X. Lei, Z. Hu, J. H. Ferris, Q. Zhang, and S. Dunn, Nano Lett. **2**, 589 (2002).

[21] Y. Tian, L. Wei, Q. Zhang, H. Huang, Y. Zhang, H. Zhou, F. Ma, L. Gu, S. Meng, L. Chen, C. Nan, and J. Zhang, Nat. Commun. **9**, 3809 (2018).

[22] D. Dahan, M. Molotskii, G. Rosenman, and Y. Rosenwaks, Appl. Phys. Lett. **89**, 152902 (2006).

[23] X. Sun, Y. J. Su, X. Li, K. W. Gao, and L. J. Qiao, J. Appl. Phys. **111**, 094110 (2012).

[24] S. Rode, R. Holscher, S. Sanna, S. Klassen, K. Kobayashi, H. Yamada, W. G. Schmidt, and A. Kuhnle, Phys. Rev. B **86**, 075468 (2012).

[25] G. Kresse and J. Furthmuller, Phys. Rev. B **54**, 11169 (1996).

[26] G. Kresse and D. Joubert, Phys. Rev. B **59**, 1758 (1999).

[27] J. P. Perdew, K. Burke, and M. Ernzerhof, Phys. Rev. Lett. **77**, 3865 (1996).

[28] J. Neugebauer and M. Scheffler, Phys. Rev. B **46**, 16067 (1992).

[29] L. Bengtsson, Phys. Rev. B **59**, 12301 (1999).

[30] S. Sanna and W. G. Schmidt, Phys. Rev. B **81**, 214116 (2010).

[31] C. Baeumer, D. Saldana-Greco, J. M. P. Martirez, A. M. Rappe, M. Shim, and L. W. Martin, Nat. Commun. **6**, 6136 (2015).

[32] R. J. Blint and M. D. Newton, J. Chem. Phys. **59**, 6220 (1973).

[33] A. L. Kholkin, I. K. Bdikin, V. V. Shvartsman, and N. A. Pertsev, Nanotechnology **18**, 095502 (2007).